The Salmonella virulence protein PagN contributes to the advent of a hyper-replicating cytosolic bacterial population

Sébastien Holbert, Emilie Barilleau, Jin Yan, Jérôme Trotereau, Michael Koczerka, Mégane Charton, Yves Le Vern, Julien Pichon, Guntram A Grassl, Philippe Velge, et al.

Virulence

ISSN: (Print) (Online) Journal homepage: www.tandfonline.com/journals/kvir20

The *Salmonella* virulence protein PagN contributes to the advent of a hyper-replicating cytosolic bacterial population

Sébastien Holbert, Emilie Barilleau, Jin Yan, Jérôme Trotereau, Michael Koczerka, Mégane Charton, Yves Le Vern, Julien Pichon, Guntram A. Grassl, Philippe Velge & Agnès Wiedemann

To cite this article: Sébastien Holbert, Emilie Barilleau, Jin Yan, Jérôme Trotereau, Michael Koczerka, Mégane Charton, Yves Le Vern, Julien Pichon, Guntram A. Grassl, Philippe Velge & Agnès Wiedemann (2024) The *Salmonella* virulence protein PagN contributes to the advent of a hyper-replicating cytosolic bacterial population, Virulence, 15:1, 2357670, DOI: 10.1080/21505594.2024.2357670

To link to this article: https://doi.org/10.1080/21505594.2024.2357670

VIRULENCE
2024, VOL. 15, NO. 1, 2357670
https://doi.org/10.1080/21505594.2024.2357670

Taylor & Francis
Taylor & Francis Group

The *Salmonella* virulence protein PagN contributes to the advent of a hyper-replicating cytosolic bacterial population

Sébastien Holbert [a], Emilie Barilleau[a], Jin Yan[b,c,d], Jérôme Trotereau[a], Michael Koczerka[a], Mégane Charton[a,e], Yves Le Vern[a], Julien Pichon [a], Guntram A. Grassl [f], Philippe Velge [a], and Agnès Wiedemann[a,b]

[a]INRAE, Université de Tours, ISP, Nouzilly, France; [b]IRSD - Institut de Recherche en Santé Digestive, ENVT, INRAE, INSERM, Université de Toulouse, UPS, Toulouse, France; [c]Department of Gastroenterology, The Second Xiangya Hospital of Central South University, China; [d]Research Center of Digestive Disease, Central South University, China; [e]Service biologie vétérinaire et santé animale, Inovalys, Angers, France; [f]Institute of Medical Microbiology and Hospital Epidemiology, Hannover Medical School and German Center for Infection Research (DZIF), Hannover, Germany

ABSTRACT

Salmonella enterica subspecies *enterica* serovar Typhimurium is an intracellular pathogen that invades and colonizes the intestinal epithelium. Following bacterial invasion, *Salmonella* is enclosed within a membrane-bound vacuole known as a *Salmonella*-containing vacuole (SCV). However, a subset of *Salmonella* has the capability to prematurely rupture the SCV and escape, resulting in *Salmonella* hyper-replication within the cytosol of epithelial cells. A recently published RNA-seq study provides an overview of cytosolic and vacuolar upregulated genes and highlights *pagN* vacuolar upregulation. Here, using transcription kinetics, protein production profile, and immunofluorescence microscopy, we showed that PagN is exclusively produced by *Salmonella* in SCV. Gentamicin protection and chloroquine resistance assays were performed to demonstrate that deletion of *pagN* affects *Salmonella* replication by affecting the cytosolic bacterial population. This study presents the first example of a *Salmonella* virulence factor expressed within the endocytic compartment, which has a significant impact on the dynamics of *Salmonella* cytosolic hyper-replication.

ARTICLE HISTORY
Received 15 December 2023
Revised 29 March 2024
Accepted 8 April 2024

KEYWORDS
Salmonella; outer membrane protein; PagN; host cell vacuole; evasion; hyper-replication

Introduction

Salmonella is a facultative intracellular entero-pathogen that has a broad host spectrum depending on its serotype and represents a risk to public health worldwide. Non-typhoidal *Salmonella* as *Salmonella enterica* subspecies *enterica serovar* Typhimurium (STm) induces asymptomatic infections in livestock, which makes it difficult to control large shedding, resulting in the contamination of water or food. Ninety-five million consumers exposed to these products developed gastroenteritis, resulting in 59,100 deaths in 2017 [1]. After ingestion, *Salmonella* survives gastric acidity and reaches the intestinal epithelium. An essential feature of *Salmonella* pathogenicity is its ability to interact with and colonize the host intestinal epithelium. This step requires invasion and intracellular replication in non-phagocytic cells, which are crucial for bacterial survival and establishment of disease in a host.

Salmonella cell invasion is dependent on the Type Three Secretion System-1 (T3SS-1) encoded by *Salmonella* Pathogenicity Island 1 (SPI-1) [2] and on two invasins, Rck [3] and PagN [4]. After internalization into host cells, *Salmonella* is contained in a unique host endocytic compartment called *Salmonella*-containing vacuole (SCV) [5]. The close cooperation of different T3SS–1 effector activities promotes SCV membrane dynamics by fusion with early endosomes and modification of lipid composition, which delays its fusion with late endosomes/lysosomes [6]. Subsequently, the migration of SCV from perinuclear localization occurs with SCV maturation into a permissive-replicative membrane-bound niche through the action of effectors secreted by the SPI-2 T3SS [7]. In the last decade, it has been established that a subset of *Salmonella* ruptures the SCV and escapes and survives in the cytosol of epithelial cells. *Salmonella* exhibits different replication rates depending on its subcellular localization. In fact, *Salmonella* undergoes hyper-replication in the cytosol, while most *Salmonella* remain within the SCV, replicating at moderate rates [8]. Remarkably, intravacuolar and cytosolic lifestyles co-exist in the same infected cells. Cytosolic hyper-replication leads to extrusion from the intestinal epithelium of host cells, allowing faecal shedding of

CONTACT Agnès Wiedemann agnes.wiedemann@inrae.fr; Sébastien Holbert sebastien.holbert@inrae.fr
Supplemental data for this article can be accessed online at https://doi.org/10.1080/21505594.2024.2357670.

Salmonella [9,10]. Deciphering the mechanisms that determine whether the internalized bacterium follows the cytosolic or intravacuolar pathway has become increasingly crucial.

The outer membrane protein PagN is encoded by the *pagN* gene, which is widely distributed and well conserved among different species and subspecies of *Salmonella* [11]. Several studies investigating *Salmonella* pathogenesis in mouse models have shown that *Salmonella pagN* invalidated exhibits reduced virulence in a mouse model of typhoid fever [12,13]. *In vitro* studies have demonstrated the role of PagN in bacterial adhesion and cellular invasion [4] and the requirement of heparan sulphate proteoglycan (HSPG) and β1 integrin (ITGB1) for these mechanisms [11,14]. *pagN* transcription is regulated by the two-component transcriptional regulatory PhoP/PhoQ system and is induced under mildly acidic pH conditions and low divalent cation concentration environments [15], conditions close to those found in the SCV. Moreover, *pagN* was upregulated in the vacuolar compartment in an infected epithelial cell model [16]. The intravacuolar expression of *pagN* along with its role in adhesion and invasion suggests that *Salmonella* prepares the vacuole to enhance its ability to reinfect other cells [11]. However, in a recent study, Galeev et al. [17] demonstrated a crucial role of proteoglycans in SCV maturation, which affects the intracellular behaviour of *Salmonella* in CHO cells [17]. Given our understanding of the relationship between HSPG and PagN, we hypothesize that PagN may have a role not only extracellularly but also intracellularly, and even more so in the SCV.

In this study, we precisely determined the localization of PagN produced by STm and investigated its role in *Salmonella* behaviour within cells. We found that PagN production mainly occurs in the SCV, and both deletion and overexpression of *pagN* significantly influenced the amount of cytosolic *Salmonella*. Our data provide strong evidence of the involvement of PagN as a precursor of cytosolic hyper-replication.

Methods

Cell lines

The Chinese Hamster ovarian cells originate from the American Type Culture Collection (CHO; ATCC: CCL-61) were cultured in DMEM (Dulbecco's modified Eagle's medium; Gibco) containing 4.5 g/L glucose supplemented with 5% foetal bovine serum (FBS; Sigma), 2 mM L-glutamine (Gibco) at 37°C and 5% CO_2 in a humidified atmosphere.

Intestinal 3D and 2D organoids derived from small intestine mice

Ileal crypts were isolated from C57 BL/6 mice and cultured as 3D organoids, as described by Suwandi *et al.* [18]. Five hundred ileal crypts embedded in 50 µL Matrigel® (Corning) in well of 24 well plate were incubated in a humidified atmosphere at 5% CO_2 and 37°C in presence of the following medium: Advanced DMEM/F12 (Gibco) supplemented with 2 mM GlutaMax (Gibco), 10 mM HEPES (Gibco), B27 1X (Gibco), 50 ng/mL mouse EGF (Sigma Aldrich), 500 nM A83–01 (Tocris), 10 µM SB202190 (Sigma Aldrich), 10 nM gastrin I (Tocris), 1 mM N-acetylcysteine (Sigma Aldrich), 10 µM Y27632 (Sigma Aldrich), and 50% supernatant of L-WRN cells (ATCC CRL-3276), containing Wnt3a, R-spondin, and Noggin as described in [19,19].

To perform infection, 2D organoid monolayers were formed from 3D organoids, as described by Suwandi *et al.* [18]. About 300–400 enteroids were dissociated and seeded onto Transwell® permeable supports (polyester membrane; 6.5 mm insert; 0.4 µm pore size; Corning) previously coated with Transwell® (diluted 1:40 in PBS) in monolayer medium containing Advanced DMEM/F-12, 2 mM GlutaMax (Gibco), 50% L-WRN-Supernatant, 20% foetal bovine serum (FBS), 50 ng/mL mouse EGF, and 10 µM dihydrochloride. The monolayer barrier integrity was estimated by measuring the transepithelial electrical resistance using Millicell-ERS (Millipore). To induce differentiation, the medium was replaced with medium containing Advanced DMEM/F-12, 2 mM GlutaMax, 5% L-WRN-Supernatant, 20% FBS, 5 µM DAPT (Tocris), and 50 ng/mL mouse EGF, and changed daily for the next 2 d.

Construction of Salmonella strains

The bacterial strains used in the present study are listed in Table 2. Chromosomal deletion of *pagN* was performed in *S.* Typhimurium ATCC 14028 STm WT strain by the λ-Red recombinant method using primers P1-PagN and P2-PagN (Table 1), as previously described [24]. The deletion mutant was verified by PCR using primers outside the deletion site.

Chromosomal gene epitope tagging by 3×FLAG epitope at the 3′ end of *pagN* gene of STm was carried out as previously described [21]. Briefly, a pair of primers was designed to amplify the 3×FLAG sequence and kanamycin resistance gene using the template plasmid pSUB11 (Tables 1 and 2). The tagged strains were then constructed using the λ-Red recombinase method [24]. The PCR product was electroporated into *Salmonella* strains carrying plasmid pKD46, and transformants were selected in the presence

Table 1. Primers used in this study.

Primer name	Sequence (5′ to 3′)
P1-3×FLAG pagN	ACACAAAGGCTGCCTCCAATGACTTCATGCTCGGCATTACTTACGCCTTTGACTACAAAGACCATGACGG
P2-3×FLAG pagN	TCCATTGCGCCTTCGGGAACCCACAGGACCAGCTATTTTACCGATAGTGTCATATGAATATCCTCCTTAG
P1-pagN	GAAACTTGTCTTTTAGCCCAATATTAAGGCAGGTTCTGAAATGAAAAACTGTGTAGGCTGGAGCTGCTTC
P2-pagN	CCTTCGGGAACCCACAGGACCAGCTATTTTACCGATAGTGTTTAAAAGGCCATATGAATATCCTCCTTAG
P1-P*pagN*-XhoI	CTCCTCGAGGCGTCAACAGGTACAACAAGATC
P2-P*pagN*-BamHI	CTCGGATCCCAAGGGGAATGATGCAGACTGCG
P1-TurboFP-START-Not1	CTCGCGGCCGCTTTAAGAAGGAGATATACATATGGGAGAG
P2-TurboFP-STOP-Not1	CTCGCGGCCGCTTAGCTGTGCCCCAGTTTGCTAGG

Table 2. Bacterial strains and plasmids used in this study.

Strain or plasmid	Relevant characteristic(s)	Source or reference
Strains		
STm WT	*S. enterica* subsp. *enterica* ser. Typhimurium ATCC 14028 wild-type strain	American Type Culture Collection
STm Δ*pagN*	14028 isogenic mutant with the *pagN* deletion (Cm^r)	This study
STm Δ*pagN* + PagN	14028 isogenic mutant with the *pagN* deletion (Cm^r) + pSUP202 containing ST 14028 *pagN* gene and its RBS (Cb^r, Tc^r)	This study
STm PagN x3FLAG	3×FLAG tag inserted at the 3′ end of the *pagN* gene of strain 14028 (Km^r)	This study
Plasmids		
pCP20	Expression of FLP recombinase and temperature-sensitive replication (Cb^r)	[20]
pSUB11	Template for construction of 3×FLAG-tagged genes (Cb^r, Km^r)	[21]
pSUP202	Cloning vector (Cb^r, Cm^r, Tc^r)	[22]
pSUP-PagN	pSUP202 containing ST 14028 *pagN* gene and its RBS (Cb^r, Tc^r)	[11]
p4889	P_{EM7}::DsRed; P_{uhpT}::sfGFP (Cb^r)	[23]
pOGV2	P_{EM7}::DsRed; P_{uhpT}::sfGFP; P_{pagN}::eqFP650 (Cb^r)	This study

of kanamycin. The strains were verified using DNA sequencing.

For plasmid construction and validation of transcriptional fusion P*pagN*::eqFP650, the plasmid pOGv2 (Supplementary Figure S1) was derived from the dual fluorescence reporter p4889 (generous gift from M. Hensel, Universität Osnabrück, Germany) by introducing a transcriptional fusion P*pagN*::eqFP650. A 410 bp promoter region of *pagN* including C-ter of STM14_0362 and N-ter of *pagN* was amplified with specific primers P1-P*pagN*-XhoI and P2- P*pagN*-BamHI (Table 1). The eqFP650 gene was amplified from plasmid pFPV-Turbo FP650 [25] using primers P1-TurboFP-START-NotI and P2-TurboFP-STOP-NotI (Table 1). After fragment amplification and intermediary subcloning in *E coli* MC1061, transcriptional fusion in p4889 was obtained and electroporated into STm WT. The plasmid was verified by sequencing and the strain was validated *in vitro*. Overnight pre-cultures in tryptic soy broth medium (TSB) of STm WT, STm WT p4889 and STm WT pOGv2 were diluted to 1/100 in low phosphate magnesium medium (LPM) containing $MgCl_2$ 8 µM (Merck), KCl 5 mM (Sigma Aldrich), NH_4SO_4 7.5 mM (UCB), K_2SO_4 0.5 mM (Merck), Glycerol 0.3% v/v (Carlo Erba), casamino acid 0.1% (Difco), H_3PO_4 337 µM (Sigma Aldrich), and 2-(N-morpholino) ethanesulfonic acid 80 mM (Sigma Aldrich) at pH 5.8 [26], or in control medium named normal phosphate magnesium medium (NPM) containing $MgCl_2$ (2 mM), KCl (5 mM), NH4SO4 (7.5 mM), K_2SO_4 (0.5 mM), Glycerol (0.3%), casamino-acid (0.1%), H_3PO_4 (25 mM), 2-(N-morpholino) ethanesulfonic acid (80 mM) at pH: 7.3, and used to inoculate a 96-well black plate (Corning). Optical density (600 nm) and fluorescence intensity analyses were performed at 15 min intervals on these cultures using a Spark Microplate Reader (TECAN) at the appropriate wavelengths to visualize eqFP650 production by incubating the plates at 37°C with shaking overnight.

The growth curve of strains STm WT, ST Δ*pagN* and STm Δ*pagN* + PagN was carried out to ensure comparable growth for all strains used. All strains were sensitive to 100 µg/mL of gentamicin (data not shown). The expression profile of PagN was evaluated for all strains in Table 2 in LB and LPM medium by Western blot (data not shown)

Bacterial infection of cells and organoid-derived monolayer

Strains were routinely grown in lysogeny broth medium (LB) at 37°C with agitation. When necessary, antibiotics were added to the culture medium at concentration of carbenicillin 100 µg/mL, kanamycin 50 µg/mL, chloramphenicol 20 µg/mL chloramphenicol. Cells were infected with bacterial strains at a multiplicity of infection (MOI) of 10 or 50, depending on experiment, for 1 h at 37°C and 5% CO2. Time zero post-infection (p.i.) was set at the beginning of the infection.

2D organoid monolayers were infected 2 days after differentiation with 2 x 10^5 STm strains using Transwell® in differentiation medium and incubated for 1 h at 37°C.

Gentamicin protection assay

For quantification of cell-associated bacteria at 1 h p.i., cells were washed four times for cells or 2 times for 2D organoid monolayers and then lysed in cold distilled H_2O for 20 min at 4°C. Finally, the number of cell-associated bacteria was determined by plating appropriate dilutions on Tryptic Soy Agar (TSA, Difco) and counting after overnight growth period at 37°C. For later time points, upon washing, medium was replaced by cell culture medium containing gentamicin (100 µg/mL, Gibco) for 1.5 h at 37°C to kill extracellular bacteria. The number of internalized bacteria was determined by plating cell lysates at 2.5 h p.i. To determine the intracellular replication level of *Salmonella* or the intracellular PagN production level in infected cells, and the intracellular localization of STm in infected cells, the cell culture medium containing gentamicin at 100 µg/mL was replaced with cell culture medium containing gentamicin at 10 µg/mL for the remaining incubation time.

Chloroquine resistance assay

To determine the number of cytosolic *Salmonella* within the cells and 2D organoid monolayers, a chloroquine (CHQ, Sigma-Aldrich) resistance assay was performed as previously described [17,27]. Briefly, the cells and 2D organoid monolayers were infected as described above. At 1.5 h and 23 h p.i., the cells were treated with CHQ (400 µM) and gentamicin (cytosolic bacteria) or with gentamicin only (total intracellular bacteria) for 1 h at 37°C. The cells were then lysed and serial dilutions were plated on TSA plates to quantify bacteria. The percentage of cytosolic bacteria corresponds to the number of live bacteria at 2.5 h or 24 h after chloroquine + gentamicin treatment compared with the number of live bacteria without chloroquine treatment at the same times expressed as a percentage.

Quantification of cells infected and cell sorting using cytometry

CHO cells were infected with STm WT p4889 strain or with STm Δ*pagN* p4889 strain at 37°C for 1 h at MOI 10:1, followed by the addition of gentamicin (100 µg/mL) for 1.5 h then followed by a further 21.5 h with gentamicin (10 µg/mL). After trypsinization, cells at 2.5 h and 24 h were analysed by flow cytometry using LSR fortessa X-20 (BD Bioscience) gated for only vacuolar bacteria (DsRed) or cytosolic bacteria (DsRed + sfGFP). Data were analysed using Kaluza software (Beckman Coulter) and the he gating strategy is illustrated (Supplementary Figure S3). The percentages of cells with cytosolic bacteria at 2.5 h p.i. and 24 h p.i. were calculated and compared between STm WT and STm Δ*pagN*.

To estimate which vacuolar or cytosolic bacteria expressed PagN, after 24 h p.i., CHO cells infected with STm PagN 3×FLAG p4889 were scraped and resuspended in cold distilled H_2O. To ensure perfect lysis, cells were passed through a 20-gauge needle 10 times on ice. The suspension was centrifuged at 200*g* 5 min at 4°C. The supernatant was collected and centrifuged again. A final centrifugation at 11,000*g* 10 min at 4°C was performed, and the pellet was resuspended in PBS 1X. Bacteria were sorted with a MoFlo Astrios EQ high-speed cell sorter (Beckman Coulter Inc., Brea, CA, USA) using morphological criteria (forward scatter and side scatter) based on the green and red fluorescence produced by bacteria.

Immunoblotting

Total protein lysates from 7.5 x 10^6 STm PagN 3×FLAG bacteria and 1.5 x 10^6 cells infected with STm PagN 3×FLAG were denatured in Laemmli sample buffer (Biorad) at the indicated time p.i. Separation of the proteins was performed using 4–15% SDS-polyacrylamide gels (Bio-rad) and transferred onto a nitrocellulose membrane (BioRad) using Trans-Blot Turbo system (BioRad). The sheets were blocked for 1 h with PBS 5% non-fat dry milk at room temperature. Detection of Hsp60 and BamB (loading control), and PagN 3×FLAG proteins was performed using respectively a polyclonal mouse anti-Hsp60 serum (Assaydesigns-Stressgen) diluted 1:6000 in PBS-Tween20 0.025% containing 0.2% non-fat dry milk; a polyclonal rabbit anti-BamB serum [28] diluted 1:6000; and monoclonal anti-FLAG M2 F1804 antibody (Sigma Aldrich) diluted 1:1000 in TBS-Tween20 0.05% plus 2% non-fat dry milk, respectively. Horseradish peroxidase (HRP)-conjugated anti-rabbit IgG (Pierce) diluted 1:25000; and anti-mouse IgG (Dako) diluted 1:5000; were used as secondary antibodies respectively in TBS-Tw20 or PBS-Tw20 plus 3% non-fat dry milk. Detection was performed by chemiluminescence using the Super Signal West Dura Extended Duration Substrate (Thermo Scientific) and Fusion FX imaging system (Vilber Lourmat).

Immunofluorescence microscopy

For subcellular *Salmonella* localisation, CHO cells were cultured on coverslips and infected with STm pOGv2 at an MOI of 50:1. Then, they were fixed at 16 h p.i. for 15 min with paraformaldehyde 4% (PFA) and stained with anti LAMP2 H4B4 (DSHB) diluted 1:40, followed by goat anti-mouse Alexa Fluor® 405 (Life Technologies) diluted 1:400.

Finally, the coverslips were mounted in a fluorescence mounting medium (Dako) ready to be imaged using confocal microscopy with a 100 × oil immersion objective (Leica TCS SP8, Germany). For quantification of cytosolic or vacuolar bacteria expressing DsRed, sfGFP and/or eqFP650. Several cells were imaged using a SP8 confocal microscope (Leica, Germany) with a water-immersion 63× objective. Bacteria characterization was performed blindly using a semi-automated macro with the Fiji software (version 1.54f, ref 1). First, all bacteria were individually segmented manually in the imaged cells. After thresholding the different fluorescent signals, these regions of interest were used to classify the cells [29]. Statistical analysis was performed using GraphPad Prism.

Infected 2D organoid monolayers were washed once time with PBS without Ca^{2+}/Mg^{2+} and fixed with PFA 4% for 20 min at room temperature. After permeabilization with PBS without Ca^{2+}/Mg^{2+} containing Triton 100X 0.5% (Sigma Aldrich), the bacteria labelling was performed with anti-*Salmonella* (Clinisciences) diluted at 1:200 in labelling buffer containing PBS with 5% goat serum (Gibco) and 3% bovine serum albumin (Sigma Aldrich) for 1 h, followed by goat-anti-rabbit Alexa Fluor® 568 (Life Technologies) diluted 1:200 in labelling buffer for 1 h to label all bacteria. Between each labelling, 2D organoid monolayers were washed three times with labelling buffer. Cytosolic bacteria were labeled with anti-GFP Alexa Fluor® 488 (Life Technologies) diluted 1:200 in labelling buffer for 1 h. Finally, nuclei were stained with DAPI (Dako) diluted 1:1000 and actin with Phalloïdin Alexa Fluor® 647 (Life Technologies) for 20 min. Images were acquired using a Leica SP8 confocal laser-scanning microscope (Leica TCS SP8, Germany).

Statistical analysis

Data were analysed using GraphPad Prism6 software (GraphPad). Statistical analysis was performed using the Mann–Whitney test, and differences among three or more groups were analysed using one-way ANOVA followed by the Kruskal–Wallis test.

Results

S. Typhimurium inside the SCV produces PagN

A tagging technique described by Uzzau et al. 2001 [21] was used to monitor PagN production under a defined set of culture conditions. We fused 3×FLAG epitope to the *pagN* gene present on the chromosome of *S.* Typhimurium 14028. Bacteria were grown in LB and LPM, the latter of which has been shown to mimic the SCV environment, that is, mild acidic pH and low divalent cation concentrations [26]. At different times of incubation, bacteria were harvested, and immunoblotting analysis was performed using specific anti-FLAG and anti-Hsp60 antibodies, a bacterial membrane protein as a protein loading control. As depicted in Figure 1, *Salmonella* maintained basal PagN production throughout the kinetics in the LB medium. However, in LPM medium, PagN production was increased compared to that in LB medium as early as 3 h in culture. This shows that *Salmonella* maximally produced PagN under acidic conditions and low concentrations of divalent cations, suggesting its production in the SCV. To verify this hypothesis, the intracellular kinetics of PagN production were monitored by immunoblotting in cells infected with STm PagN 3×FLAG. CHO cells were chosen as they were previously used to study the role of PagN in *Salmonella* invasion mechanism [4]. The bacteria in LB medium, as shown in Figure 1, as well as the inoculum and non-internalized bacteria, did not produce PagN (Figure 2). On the other hand, from 2.5 h and up to 24 h, intracellular *Salmonella* produced increasing amounts of PagN (Figure 2). Based on the previously described plasmid p4889 (Röder 2020) [23], which allows discrimination between vacuolar and cytosolic *Salmonella*, the

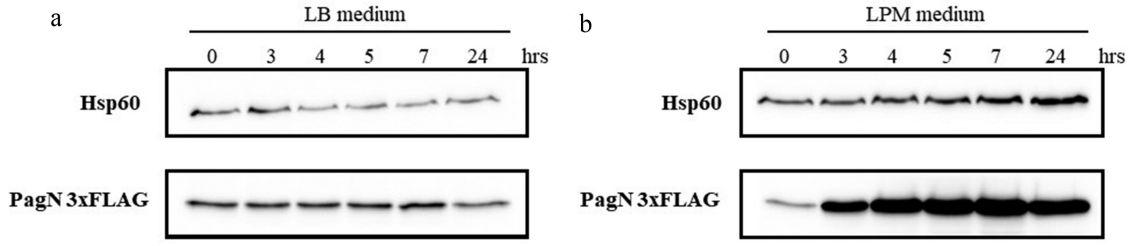

Figure 1. PagN production is induced under culture conditions mimicking the intravacuolar lifestyle of *Salmonella*. Production of PagN 3×FLAG in STm WT after culture (a) in LB or (b) in LPM was estimated. 2 x 10^8 bacteria were denatured and the protein level and the production of PagN was verified by Western blotting as described in Methods. The images are representative of two independent experiments.

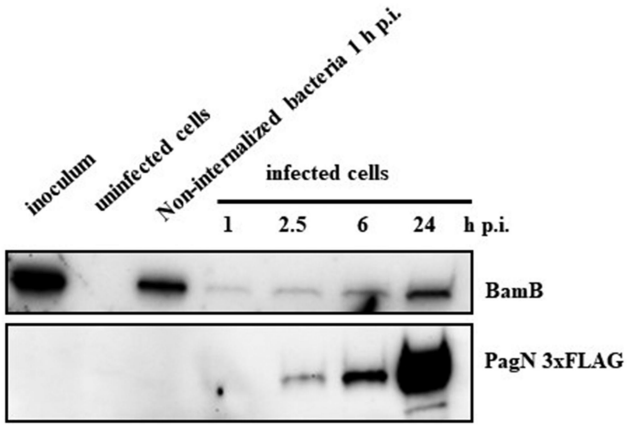

Figure 2. PagN is produced during CHO cells infection. CHO cells were infected with STm PagN x3FLAG at MOI 50:1 for 1 h at 37 °C followed by 1 h with gentamicin 100 µg/mL and extra time with gentamicin 10 µg/mL corresponding to 2.5, 6 and 24 h p.i. At the indicated time, Laemmli buffer resuspension of the bacterial inoculum (representing 1.5 x 10^6 bacteria in 10 µL), of the uninfected or of cell culture supernatant containing extracellular bacteria 1 h p.i. Or of the infected cells were loaded as described in Methods. The bacterial protein level BamB and the production of PagN have been verified by immunoblotting. The image is representative of three independent experiments.

construction of the plasmid pOGv2 (Supplementary Figure S1) allows the assessment of the conditions of *pagN* transcription by production of fluorescent protein eqFP650 under the control of the P_{pagN} promoter in synthetic NPM and LPM medium (Figure 3a) and in CHO cells (Figure 3b). NPM was developed from LPM and used instead of LB because LB induces weak autofluorescence that interferes with fluorochrome analysis (data not shown). To estimate *pagN* transcription kinetics, the relative intensity of eqFP650 fluorescence of measured OD600 nm liquid culture of STm WT, STm WT p4889, and STm WT pOGv2 were recorded using a Tecan Fluorescence microplate reader (Figure 3a). Transcription of *pagN* was observed only in LPM medium. In CHO cells, *pagN* transcription confirmed by eqFP650 production was only induced by bacteria embedded in LAMP2 positive SCV unlike free cytosolic bacteria that transcribed *uhpT* allowing GFP production (Figure 3b,c). To ensure that the intravacuolar transcription of *pagN* leads to PagN production, cell sorting of bacteria from CHO cells infected with STm PagN 3×FLAG p4889 was performed on the basis of their fluorescence: i) bacteria only red were vacuolar and ii) bacteria red and green were cytosolic. Bacteria were harvested and immunoblotting analysis was performed using specific anti-FLAG and anti-BamB antibodies. The results shown in Figure 4 confirm that PagN production by *Salmonella* is highly increased in SCV, with residual production by cytosolic bacteria. Altogether, our results demonstrate that PagN is produced mainly by STm when bacteria reside in the SCV.

PagN impacts the intracellular replication of Salmonella*, by facilitating hyper-replication*

Currently, three distinct survival states have been described for *Salmonella*: dormancy within vesicular compartments, replication within the SCV, and hyper-replication in the cytosol, as described in previous studies [27,30,31]. To facilitate replication, *Salmonella* hijacks its host cell machinery. Key factors in maintaining replication within vacuoles include the T3SS–1 and T3SS–2 effectors. Notably, the vacuolar production of PagN under conditions similar to those of T3SS–2 led us to investigate its role in *Salmonella's* intracellular replication. To assess intracellular replication, a Δ*pagN* mutant (STm Δ*pagN*) and complemented strain (STm Δ*pagN* + PagN) were constructed. Before exploring the potential role of PagN in replication and considering that PagN has been characterized as an invasion factor for specific cells, we assessed the ability of *Salmonella* wild-type and mutant strains to adhere to and invade CHO cells (Supplementary Figure S2). Adhesion assays showed that *pagN* deletion did not affect bacterial adhesion (Supplementary Figure S2A). These results could be related to the fact that PagN was produced at a low level under our *in vitro* LB culture conditions (Figure 1). However, the fact that the complemented strain with a plasmid carrying *pagN* has higher adhesion and internalization ability than the STm Δ*pagN* mutant strain confirms the contribution of PagN in *S.* Typhimurium adhesion and internalization (Supplementary Figure S2 A-B). In this context, we examined whether PagN influences the replication of intracellular *Salmonella*. A combination of gentamicin and chloroquine resistance assays was performed in CHO cells infected with STm WT, STm Δ*pagN* and complemented Δ*pagN* + PagN strains at 2.5 h and 24 h p.i. As chloroquine, together with gentamicin, is known to kill *Salmonella* only inside the SCV [27], this assay allows quantification of the percentage of cytosolic bacteria in the total intracellular bacterial population. At 2.5 h p.i., infection of CHO cells with the ST Δ*pagN* mutant had no impact on the cytosolic share compared with the ST WT (Figure 5a). However, overexpression of *pagN* induced a significant increase in the proportion of cytosolic bacteria from 2.5 h p.i. (Figure 5a). At 24 h p.i., the

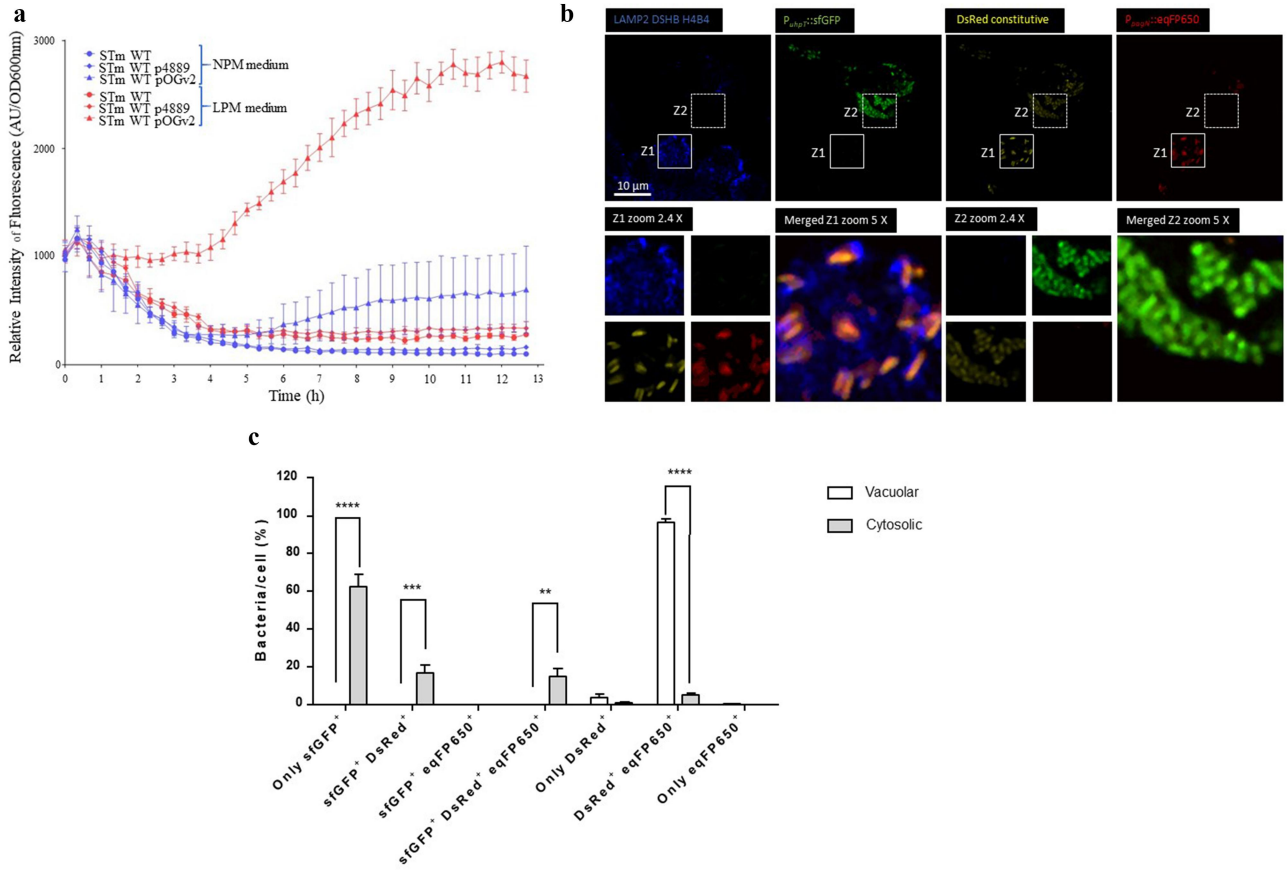

Figure 3. PagN is produced in the SCV. (a) STm WT, STm WT p4889 and STm WT pOGv2 were cultured in (blue marks) medium with normal concentration of phosphate and magnesium and neutral pH named NPM or were cultured in (red marks) LPM medium with low concentration of phosphate and magnesium and acidic pH (5.8). To estimate *pagN* transcription at the indicated time (hours) relative intensity of eqFP650 fluorescence of measured OD600nm liquid cultured of (dot) STm WT, (square) STm WT p4889 and (triangle) STm WT pOGv2 were recorded with Tecan Fluorescence microplates reader. (b) CHO cells were infected with STm WT pOGv2 at MOI 50:1 for 1 h at 37°C followed by 1 h with gentamicin 100 µg/mL and extra time with gentamicin 10 µg/mL correspond to 24 h p.i. then fixed and stained with mouse LAMP2 antibody, then revealed with anti-mouse Alexa Fluor 405 (blue). Imaging was performed using confocal microscopy with a 100 × oil immersion objective (Leica TCS SP8, Germany). Vacuolar spaces were LAMP2 positive (blue) vacuolar *Salmonella* were visualized in yellow (DsRed constitutive: yellow), hyper replicative cytosolic *Salmonella* were observed red and weakly yellow (sfGFP inducible: green and DsRed constitutive: weakly yellow due to hyper replication), and *Salmonella* P*pagN* transcriptionnaly active were red (P*pagN*::eqFP650: red). Continuous white square named Z1 representing vacuolar bacteria or dashed white square named Z2 representing cytosolic bacteria were oversized 2.4 times and 5 times for merged images. Scale bars 10 µm. (c) Quantification of vacuolar or cytosolic *Salmonella* with P*pagN* transcriptionnaly active from CHO cells infected with STm WT pOGv2 at MOI 50:1 for 1 h at 37°C followed by 1 h with gentamicin 100 µg/mL and extra time with gentamicin 10 µg/mL correspond to 24 h p.i. then fixed. Images obtained using confocal microscopy with a water-immersion 63× objective (Leica TCS SP8, Germany) were analyzed with a script described in Methods.

infection of CHO cells with the STm Δ*pagN* mutant resulted in a smaller cytosolic bacterial population than that of the wild-type strain. In addition, the observation made with the strain overexpressing *pagN* at 2.5 h p.i. was confirmed by a very significant increase in the proportion of cytosolic bacteria at 24 h p.i (Figure 5b). The ratio of the number of internalized bacteria at 24 h p.i. and 2.5 h p.i. allows the calculation of the bacterial replication rate. As shown in Figure 5c, the STm Δ*pagN* had a significantly lower bacterial replication rate (approximately 40%) compared to the wild-type strain. The complemented strain restored its replication rate to that of the wild-type strain. Another way to estimate the impact of PagN on the intracellular localization of *Salmonella* is to use flow cytometry and the p4889 tool to quantify infected cells harbouring cytosolic bacteria, that is, cells that are both red and green. At 2.5 h p.i., no difference was observed between STm WT and STm Δ*pagN* in cells harbouring cytosolic bacteria (Figure 6a). At 24 h p.i., the STm Δ*pagN* strain showed a decrease in the percentage of cytosolic bacteria compared to the percentage obtained with the STm WT (Figure 6b).

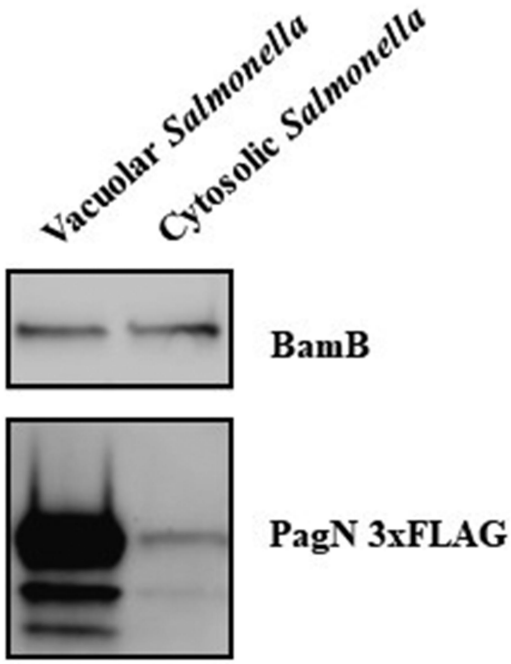

Figure 4. PagN is produced in SCV during CHO cells infection. CHO cells were infected with STm PagN x3FLAG p4889 at MOI 50:1 for 1 h at 37°C followed by 1 h with gentamicin 100 µg/mL and extra time with gentamicin 10 µg/mL corresponding to 24 h p.i. At the indicated time, cells were lysed and *Salmonella* were rescued and sorted by Fluorescence-activated cell sorting. Two populations were sorted *Salmonella* DsRed without sfGFP (vacuolar *Salmonella*) and DsRed with GFP (cytosolic *Salmonella*). Then, 15 µL over 100 µL of Laemmli buffer resuspension (representing 3 x 10^5 bacteria) were loaded as described in Methods. The bacterial protein level BamB and the production of PagN have been verified by immunoblotting. These images are representative of two independent experiments.

PagN influences S. Typhimurium intracellular behavior in organoid-derived intestinal epithelial monolayer

To further investigate whether PagN influences STm intracellular behaviour in the intestinal epithelium, *in vitro* mouse intestinal organoids were derived from the ileal crypts and cultivated as 3D organoids. These 3D organoids were dissociated and seeded onto Transwell® permeable supports to form 2D organoid monolayers. Polarized 2D organoid monolayers were infected with STm WT, Δ*pagN* mutant, or complemented Δ*pagN* + PagN strains to quantify the number of internalized bacteria after 1 h of infection, the bacterial replication rate, and the number of cytosolic bacteria after 24 h of infection. As shown in Figure 7, despite no significant difference in internalization of STm WT and *pagN* mutant strains at 2.5 h p.i., the *pagN* absence considerably reduces bacterial replication and the number of cytosolic bacterial load at 24 h p.i. In addition, *pagN* overexpression in the STm-complemented Δ*pagN* + PagN strain significantly increased the levels of infection, bacterial replication, and cytosolic bacteria compared to the STm *pagN* mutant strain. Moreover, a 2D organoid monolayer infected with STm WT p4889 allowed us to visualize the presence of vacuolar and cytosolic bacteria, as observed in CHO cell lines (Figure 8). Taken together, our data obtained with the CHO cell line were reproduced in *in vitro* intestinal epithelium.

Collectively, these data allow us to conclude that, in addition to its role as an invasin, PagN contributes to *Salmonella* intracellular hyper-replication, suggesting a role in vacuolar escape of the bacterium to the host cytosol.

Discussion

Following STm invasion of epithelial cells, intracellular bacteria survive and replicate within two distinct niches, intravacuolar and cytosolic. *Salmonella* residing in the cytosolic niche replicates faster than in the intravacuolar niche [27,32]. The T3SS–1 and T3SS–2 effectors are implicated in intracellular survival. There is a chronology of events related to the temporal expression of T3SS–1 and T3SS–2 in intracellular *Salmonella*. T3SS–1 and its effectors are key factors in the invasion process; immediately after invasion, they can be a source of very early instability. Indeed, translocon proteins and effectors of T3SS–1 are active in maintaining SCV integrity [33–35]. During SCV maturation, effectors of T3SS–2 play a role in SCV stability [36,37]. Indeed, the absence of specific T3SS–2 effectors leads to SCV destabilization. The action of T3SS–2 effectors favours the preservation of the integrity of the SCV, as illustrated by the complex action of SifA in *Salmonella* virulence [38]. SCV instability leading to hyper-replicative cytosolic *Salmonella* is rare, representing less than 10% of infected cells [27]. However, T3SS–1 is substantially upregulated in hyper-replicating bacteria [16] providing them with a significant advantage in the dynamics of intestinal dissemination [9]. Furthermore, host factors such as TBK1 kinase, guanylate-binding proteins or the COPII complex play crucial roles in maintaining vacuolar integrity [39–41]. The balance between *Salmonella* and its hosts is dynamic. An action by one partner triggers a response from the other, which, in turn, adapts. The events leading to vacuolar destabilization and escape from the intravacuolar niche still require further investigation. These

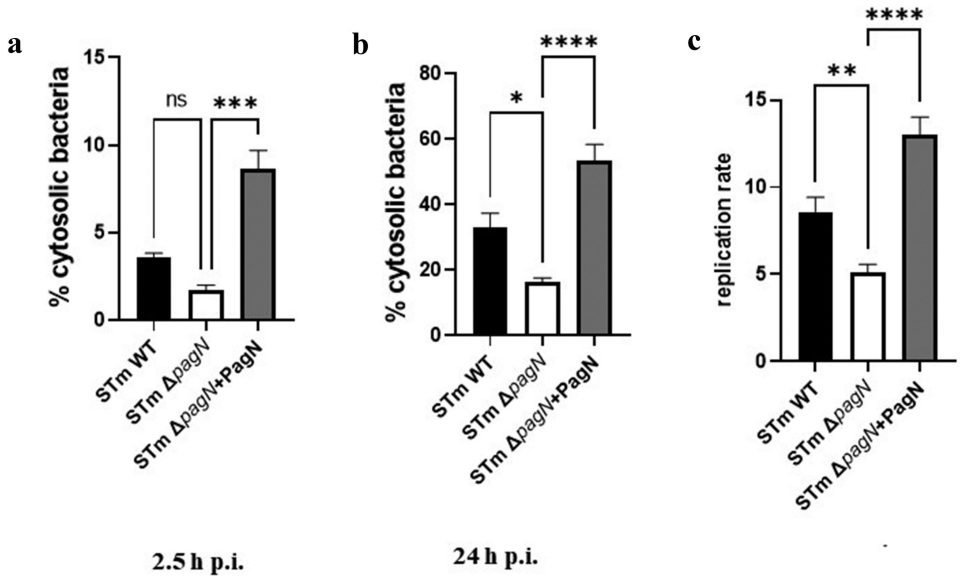

Figure 5. PagN leads to the cytosolic presence of *Salmonella*. CHO cells were infected (black bars) with STm WT or (empty bars) with STm Δ*pagN* strain or (grey bars) with STm Δ*pagN* + PagN complemented (pSUP202 *pagN*) at 37 °C for 1 h at MOI 10:1, (a) followed by the addition of gentamicin (100 µg/mL) added to chloroquine (400 µM) for 1.5 h or (b) followed by a further 21.5 h with gentamicin (10 µg/mL) added to chloroquine (400 µM) 1 h before the end of experiment. The percentage of cytosolic bacteria (a) at 2.5 h p.i. And (b) at 24 h p.i. and (c) the replication rate has been calculated as described in Methods. Data show mean values ± SEM acquired from three independent experiments with three infected wells per experiment. (****$p < 0.0001$, ***$p < 0.001$, **$p < 0.01$, *$p < 0.05$, ns: non-significant).

studies suggest that several players expressed by *Salmonella* in SCV or host factors contribute to the advent of a hyper-replicating cytosolic bacterial population. Can PagN be a bacterial factor?

Here, we explored the function of PagN in intracellular *Salmonella* behaviour. PagN is an outer membrane protein implicated in *Salmonella* adhesion and the invasion of non-phagocytic cells [4]. More specifically, PagN requires HSPG associated with the ITGB1 receptor, allowing PagN-mediated internalization in multiple cell lines such as CHO, HT29, RKO, and IPEC-J2 cells [4,11,14,42]. It contributes to the actin cytoskeleton and membrane rearrangement, which are required for bacterial invasion [11]. In this study, we confirmed that *pagN* expression and PagN production are favoured under vacuolar-like conditions in synthetic medium with mild acidic pH and low Mg^{2+} concentration, but also in cellular models that the *pagN* expression and PagN production are favoured in vacuolar-like conditions. The production of PagN at 2.5 h was strongly increased at 6 h and even higher at 24 h. After 6 h of infection, the SCV is considered mature, allowing intravacuolar *Salmonella* replication [43]. The increase in the bacterial population within the vacuole partly accounted for the increase in the quantity of PagN detected. Indeed, even if the production of PagN is mainly observed in vacuolar bacteria, the residual production of cytosolic bacteria remains. Moreover, *pagN* invalidation leads to fewer cytosolic bacteria at the late stage of infection, and the overproduction of PagN induces a higher number of cytosolic bacteria. Vacuolar production of PagN consequently influences its intracellular survival by promoting a hyper-replicating cytosolic population.

The composition of the inner membrane of the SCV contains molecules that are natively observed on the cell surface, among other proteoglycans and ITGB1 [44]. Proteoglycans play a crucial role in the PIKfyve-dependent endolysosomal fusion process, which has been shown to impact intracellular *Salmonella* survival [17]. We propose that PagN production within the *Salmonella*-containing SCV leads to an increased reliance on HSPG. This reliance may disrupt the normal interaction between PIKfyve and proteoglycans, consequently dysregulating endolysosomal fusion. Such dysregulation could facilitate the escape of *Salmonella* from the SCV. Another hypothesis can be proposed based on behaviour of *Yersinia* in its vacuole. *Yersinia pseudotuberculosis* produces a toxin known as cytotoxic necrotizing factor. This toxin gains access to the cytosol of target cells through its close interaction with HSPGs and a modification linked to acidification of the endosome in which it resides [45]. The escape mechanism is not well understood, but it results in destabilization of the endosomal membrane. The production of PagN by *Salmonella* in SCV acidified in proximity to HSPG

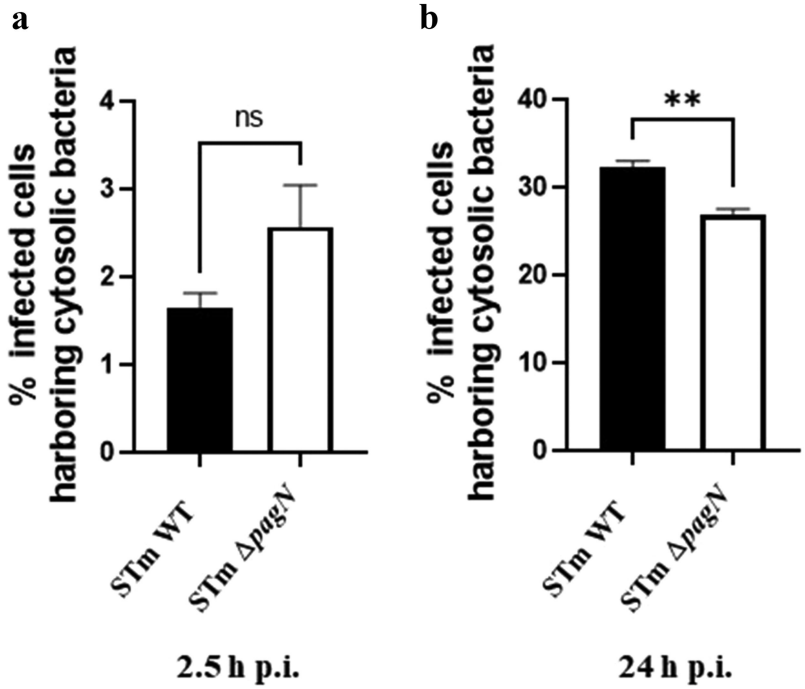

Figure 6. PagN acts on the late cytosolic fate of *S.* Typhimurium in CHO cells. CHO cells were infected with STm WT p4889 strain (black bars) or with STm Δ*pagN* p4889 strain (white bars) at 37 °C for 1 h at MOI 10:1 followed by the addition of gentamicin (100 µg/mL) for 1.5 h then followed by a further 21.5 h with gentamicin (10 µg/mL). After trypsinization, cells at (a) 2.5 h and (b) 24 h p. i. were analysed by flow cytometry gated for only vacuolar bacteria (DsRed) or cytosolic bacteria (DsRed + sfGFP). The percentage of cells with cytosolic bacteria at 2.5 h p.i. and at 24 h p.i. has been calculated and compared between STm WT and STm Δ*pagN*. Data show mean values ± SEM acquired from three independent experiments with three infected wells per experiment. (**$p < 0.01$, ns: non-significant).

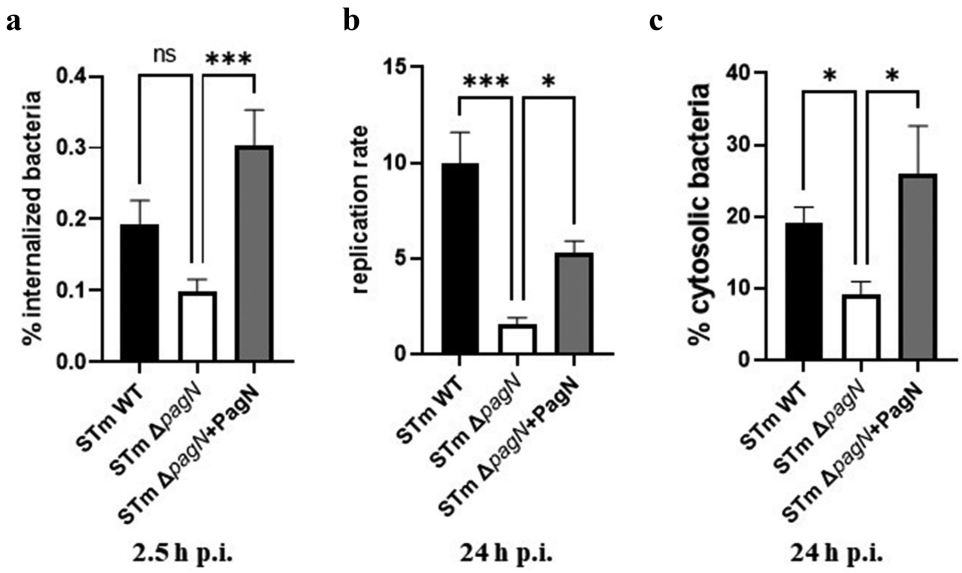

Figure 7. PagN production affects *S.* Typhimurium intracellular replication and localization within intestinal epithelium. 3D organoids were dissociated, seeded on Transwell® permeable supports and grown into a differentiated 2D organoid monolayer. 2D organoid monolayers were infected with STm WT, Δ*pagN* mutant or with the STm Δ*pagN* + PagN complemented (pSUP202 *pagN*) strains for 1 h. Quantification of (a) the percentage of internalized bacteria at 2.5 h p.i., (b) the bacterial replication level and (c) the percentage of cytosolic bacteria at 24 h p.i. per Transwell®. Graphs show the mean ± SEM of at least two independent experiments with four Transwells® evaluated for each experiment (***$p < 0.001$, *$p < 0.05$, ns: non-significant).

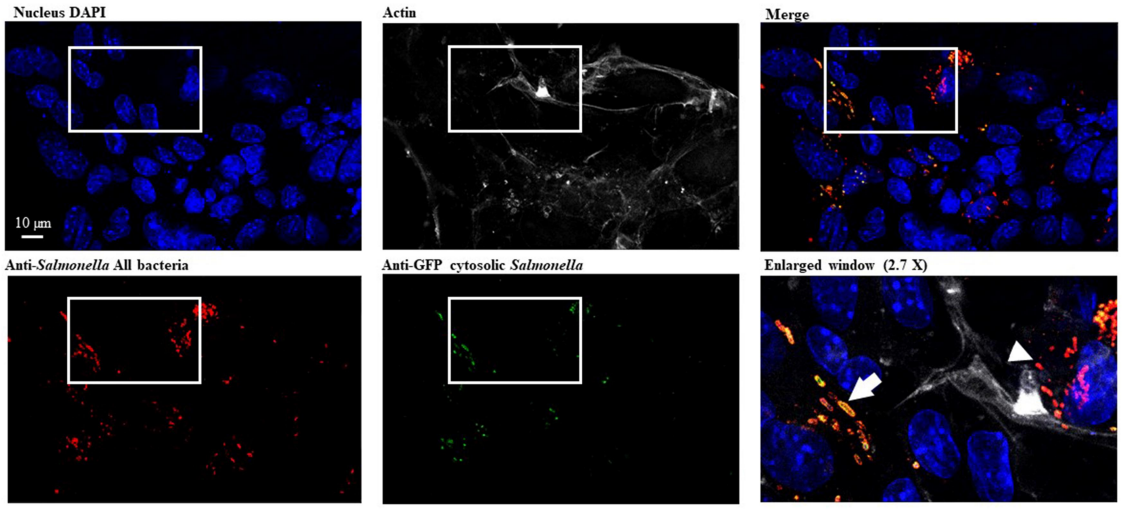

Figure 8. *S.* Typhimurium intracellular localization within intestinal epithelium. 3D organoids were dissociated, seeded on Transwell® permeable supports and grown into a differentiated 2D organoid monolayer. 2D ileum organoïds were infected with STm WT p4889 for 1.5 h at 37 °C followed by 1.5 h with gentamicin 100 µg/mL and extra time with gentamicin 10 µg/mL correspond to 24 h p. i. then fixed and stained with DAPI for nucleus (blue), Phalloïdin Alexa Fluor 647 for actin (grey), *Salmonella* antibody detected with goat anti-rabbit Alexa Fluor 568 (red) and anti-GFP conjugated Alexa Fluor 488 (green). Imaging was performed using confocal microscopy with a water-immersion 63× objective (Leica TCS SP8, Germany). On three time enlarged window vacuolar *Salmonella* were visualized red targeted by white arrow head (DsRed constitutive: red) and hyper-replicative cytosolic *Salmonella* were observed mixed red/yellow targeted by white arrow (corresponding to colocalization of sfGFP inducible (green) and DsRed constitutive (red)). Scale bar 10 µm.

could trigger this process, leading to the presence of cytosolic bacteria. Concerning ITGB1, the adhesins *Neisseria meningitidis* NadA, *Yersinia adhesin* YadA, and invasin Inv, along with *Salmonella* PagN, rely on ITGB1 to fulfill their invasin functions [11,46,47]. Among the bacterial pathogens known to escape their vacuoles, integrins are not currently used for this process. However, in the same way as HSPG, ITGB1 is subjected through its endosomal pathway to recycling or to a lysosomal degradation. Sorting nexin 17 (SNX) interacts with the ITGB1 cytoplasmic tail, which contributes to its recycling. Several SNX proteins, such as SNX1 [48], SNX3 [49] and SNX18 [50] have been implicated in SCV maturation. Through an as-yet-undetermined mechanism, PagN may interfere with this signalling pathway, imposing a potential ITGB1-dependent influence on SCV maturation, which could lead to the presence of bacteria within the cytosol.

If we exclude *Salmonella*, the escape mechanism of which is yet to be deciphered, several pathogens are known to escape from their vacuole, such as *Listeria monocytogenes*, *Shigella flexneri* and *Mycobacterium tuberculosis*. *Listeria monocytogenes* destabilizes vacuole membranes using the pore-forming toxin listeriolysin O and two phospholipases, PlcA and PlcB [51–53]. *Shigella flexneri* translocates a T3SS effector, IpgD, that initiates a cascade of host phosphoinositide signalling, disrupting the endosomal process and ultimately causing vacuole disintegration (Chang 2020) [54]. *Mycobacterium tuberculosis* relies on the biosynthesis and transport of the cell wall lipid phthiocerol dimycocerosates to escape from vacuoles, the molecular mechanism of which requires further investigation [55]. PagN, an outer membrane protein, appears to have no apparent similarities with the previously mentioned escape actor proteins. A search for homology in databases with proteins from other bacteria does not yield information regarding its function beyond its role as an adhesin. Current investigations aim to elucidate the molecular mechanisms triggered by PagN and its specific role in cytosolic replication.

Overall, our results allowed us to propose a new model of the intestinal infectious cycle for STm involving PagN. *Salmonella* invades the epithelium from the apical side and resides in the SCV. Once inside the host cell, there is considerable heterogeneity in the outcome of infection. From 4 to 6 h p.i., some bacteria start replicating within the SCV following a well-described process involving T3SS–2 effectors [43] and a bacterial population is released into the cytosol and hyper-replicated [27]. How this vacuolar escape occurs remains to be clarified. Consequently of its intracellular survival, *Salmonella* may behave differently: (i) *Salmonella* can cross the intestinal barrier and exit on the basolateral side [56], and (ii) cells containing hyper-

replicative cytosolic bacteria are extruded from the monolayer, releasing bacteria from the apical side [9]. Sloughing of enterocytes laden with *Salmonella* from villus tips has been observed *in vivo* and *in vitro* [10,57]. In addition, Knodler *et al.* showed that *Salmonella* released from these cells are invasion-primed [9,10]. It can, therefore, be assumed that *Salmonella* that emerges from epithelial cells could facilitate subsequent interactions with mammalian cells that the bacteria encounter, facilitating *Salmonella* colonization. In this study, we observed cell extrusion of infected cells in the CHO model and 2D organoid monolayers, which we did not quantify. This oversight likely resulted in an underestimation of the effect of PagN on vacuolar escape. However, we did not assess the direct impact of PagN on the inflammasome or cell viability. Ongoing and future studies will provide insights into the specific role of PagN and its interactions with cellular partners in epithelial destabilization and *Salmonella* shedding.

Acknowledgements

We thank M. Hensel (Universität Osnabrück, Germany) for generously providing the dual fluorescence reporter p4889 (Roder and Hensel 2020). Jin Yan holds a doctoral fellowship, granted by the China Scholarship Council. Michael Koczerka holds a doctoral fellowship at the University of Tours (France).

Disclosure statement

No potential conflict of interest was reported by the author(s).

Funding

The author(s) reported that there is no funding associated with the work featured in this article.

Author contributions

AW designed the study; EB, JT, MK, and MC designed the tools. SH, EB, JY, MK, YLV, JP and AW performed the research; SH, GG, and AW analysed the data; AW and SH wrote the manuscript; PV and GG provided critical comments. All the authors have read and approved the final manuscript.

Data availability statement

The authors confirm that the data supporting the findings of this study are available in the article and its supplementary materials or by consulting this link https://doi.org/10.57745/W1XELF.

ORCID

Sébastien Holbert http://orcid.org/0000-0001-7655-3144
Julien Pichon http://orcid.org/0000-0002-2885-5903
Guntram A. Grassl http://orcid.org/0000-0003-3718-2090
Philippe Velge http://orcid.org/0000-0002-8201-0194

References

[1] Collaborators GBDCOD. Global, regional, and national age-sex-specific mortality for 282 causes of death in 195 countries and territories, 1980-2017: a systematic analysis for the global burden of disease study 2017. Lancet. 2018;392(10159):1736–1788.
[2] Hong KH, Miller VL. Identification of a novel salmonella invasion locus homologous to Shigella ipgDE. J Bacteriol. 1998;180(7):1793–1802.
[3] Rosselin M, Virlogeux-Payant I, Roy C, et al. Rck of Salmonella enterica, subspecies enterica serovar enteritidis, mediates zipper-like internalization. Cell Res. 2010;20(6):647–664.
[4] Lambert MA, Smith SG. The PagN protein of Salmonella enterica serovar typhimurium is an adhesin and invasin. BMC Microbiol. 2008;8:142.
[5] Garcia-Del Portillo F, Foster JW, Maguire ME, et al. Characterization of the micro-environment of salmonella typhimurium-containing vacuoles within MDCK epithelial cells. Mol Microbiol. 1992;6(22):3289–3297.
[6] Lau N, Haeberle AL, O'Keeffe BJ, et al. SopF, a phosphoinositide binding effector, promotes the stability of the nascent salmonella-containing vacuole. PLOS Pathog. 2019;15(7):e1007959.
[7] LaRock DL, Chaudhary A, Miller SI. Salmonellae interactions with host processes. Nat Rev Microbiol. 2015;13(4):191–205.
[8] Knodler LA. Salmonella enterica: living a double life in epithelial cells. Curr Opin Microbiol. 2015;23:23–31.
[9] Chong A, Cooper KG, Kari L, et al. Cytosolic replication in epithelial cells fuels intestinal expansion and chronic fecal shedding of salmonella typhimurium. Cell Host Microbe. 2021;29(7):1177–1185 e1176.
[10] Knodler LA, Vallance BA, Celli J, et al. Dissemination of invasive Salmonella via bacterial-induced extrusion of mucosal epithelia. Proc Natl Acad Sci U S A. 2010;107(41):17733–17738.
[11] Barilleau E, Vedrine M, Koczerka M, et al. Investigation of the invasion mechanism mediated by the outer membrane protein PagN of salmonella typhimurium. BMC Microbiol. 2021;21(1):153.
[12] Conner CP, Heithoff DM, Mahan MJ. In vivo gene expression: contributions to infection, virulence, and pathogenesis. Curr Top Microbiol Immunol. 1998;225:1–12.
[13] Yang Y, Wan C, Xu H, et al. Identification of an outer membrane protein of salmonella enterica serovar typhimurium as a potential vaccine candidate for salmonellosis in mice. Microbes Infect. 2013;15(5):388–398.
[14] Lambert MA, Smith SG. The PagN protein mediates invasion via interaction with proteoglycan. FEMS Microbiol Lett. 2009;297(2):209–216.

[15] Belden WJ, Miller SI. Further characterization of the PhoP regulon: identification of new PhoP-activated virulence loci. Infect Immun. 1994;62(11):5095–5101.
[16] Powers TR, Haeberle AL, Predeus AV, et al. Intracellular niche-specific profiling reveals transcriptional adaptations required for the cytosolic lifestyle of salmonella enterica. PLOS Pathog. 2021;17(8):e1009280.
[17] Galeev A, Suwandi A, Bakker H, et al. Proteoglycan-dependent endo-lysosomal fusion affects intracellular survival of salmonella typhimurium in epithelial cells. Front Immunol. 2020;11:731.
[18] Suwandi A, Alvarez KG, Galeev A, et al. B4galnt2-mediated host glycosylation influences the susceptibility to citrobacter rodentium infection. Front Microbiol. 2022;13:980495.
[19] Lacroix-Lamande S, Bernardi O, Pezier T, et al. Differential salmonella typhimurium intracellular replication and host cell responses in caecal and ileal organoids derived from chicken. Vet Res. 2023;54(1):63.
[20] Cherepanov PP, Wackernagel W. Gene disruption in Escherichia coli: TcR and KmR cassettes with the option of Flp-catalyzed excision of the antibiotic-resistance determinant. Gene. 1995;158(1):9–14.
[21] Uzzau S, Figueroa-Bossi N, Rubino S, et al. Epitope tagging of chromosomal genes in salmonella. Proc Natl Acad Sci USA. 2001;98(26):15264–15269.
[22] Simon R, Priefer U, Pühler A. A broad host range mobilization system for in vivo genetic engineering: transposon mutagenesis in gram negative bacteria. Bio/Technol. 1983;1:784–791.
[23] Roder J, Hensel M. Presence of SopE and mode of infection result in increased salmonella-containing vacuole damage and cytosolic release during host cell infection by salmonella enterica. Cell Microbiol. 2020;22(5):e13155. doi: 10.1111/cmi.13155
[24] Datsenko KA, Wanner BL. One-step inactivation of chromosomal genes in Escherichia coli K-12 using PCR products. Proc Natl Acad Sci USA. 2000;97(12):6640–6645.
[25] Roche SM, Holbert S, Le Vern Y, et al. A large panel of chicken cells are invaded in vivo by salmonella typhimurium even when depleted of all known invasion factors. Open Biol. 2021;11(11):210117.
[26] Coombes BK, Brown NF, Valdez Y, et al. Expression and secretion of salmonella pathogenicity island-2 virulence genes in response to acidification exhibit differential requirements of a functional type III secretion apparatus and SsaL. J Biol Chem. 2004;279(48):49804–49815.
[27] Knodler LA, Nair V, Steele-Mortimer O. Quantitative assessment of cytosolic salmonella in epithelial cells. PLOS ONE. 2014;9(1):e84681.
[28] Namdari F, Hurtado-Escobar GA, Abed N, et al. Deciphering the roles of BamB and its interaction with BamA in outer membrane biogenesis, T3SS expression and virulence in salmonella. PLOS ONE. 2012;7(11):e46050.
[29] Schindelin J, Arganda-Carreras I, Frise E, et al. Fiji: an open-source platform for biological-image analysis. Nat Methods. 2012;9(7):676–682.
[30] Luk CH, Valenzuela C, Gil M, et al. Salmonella enters a dormant state within human epithelial cells for persistent infection. PLOS Pathog. 2021;17(4):e1009550.
[31] Steele-Mortimer O, Brumell JH, Knodler LA, et al. The invasion-associated type III secretion system of salmonella enterica serovar typhimurium is necessary for intracellular proliferation and vacuole biogenesis in epithelial cells. Cell Microbiol. 2002;4(1):43–54.
[32] Malik-Kale P, Winfree S, Steele-Mortimer O. The bimodal lifestyle of intracellular salmonella in epithelial cells: replication in the cytosol obscures defects in vacuolar replication. PLOS ONE. 2012;7(6):e38732.
[33] Brumell JH, Tang P, Zaharik ML, et al. Disruption of the Salmonella-containing vacuole leads to increased replication of Salmonella enterica serovar typhimurium in the cytosol of epithelial cells. Infect Immun. 2002;70(6):3264–3270.
[34] Du J, Reeves AZ, Klein JA, et al. The type III secretion system apparatus determines the intracellular niche of bacterial pathogens. Proc Natl Acad Sci USA. 2016;113(17):4794–4799.
[35] Thurston TL, Wandel MP, von Muhlinen N, et al. Galectin 8 targets damaged vesicles for autophagy to defend cells against bacterial invasion. Nature. 2012;482(7385):414–418.
[36] Brumell JH, Goosney DL, Finlay BB. SifA, a type III secreted effector of salmonella typhimurium, directs salmonella-induced filament (Sif) formation along microtubules. Traffic. 2002;3(6):407–415.
[37] Ruiz-Albert J, Yu XJ, Beuzon CR, et al. Complementary activities of SseJ and SifA regulate dynamics of the salmonella typhimurium vacuolar membrane. Mol Microbiol. 2002;44(3):645–661.
[38] Zhao W, Moest T, Zhao Y, et al. The salmonella effector protein SifA plays a dual role in virulence. Sci Rep. 2015;5:12979.
[39] Meunier E, Dick MS, Dreier RF, et al. Caspase-11 activation requires lysis of pathogen-containing vacuoles by IFN-induced GTPases. Nature. 2014;509(7500):366–370.
[40] Radtke AL, Delbridge LM, Balachandran S, et al. TBK1 protects vacuolar integrity during intracellular bacterial infection. PLOS Pathog. 2007;3(3):e29.
[41] Santos JC, Duchateau M, Fredlund J, et al. The COPII complex and lysosomal VAMP7 determine intracellular salmonella localization and growth. Cell Microbiol. 2015;17(12):1699–1720.
[42] Wu Y, Hu Q, Dehinwal R, et al. The not so good, the bad and the ugly: differential bacterial adhesion and invasion mediated by salmonella PagN allelic variants. Microorganisms. 2020;8(4):489. https://doi.org/10.3390/microorganisms8040489
[43] Steele-Mortimer O. The salmonella-containing vacuole: moving with the times. Curr Opin Microbiol. 2008;11(1):38–45.
[44] Garcia-Del Portillo F, Pucciarelli MG, Jefferies WA, et al. Salmonella typhimurium induces selective aggregation and internalization of host cell surface proteins during invasion of epithelial cells. J Cell Sci. 1994;107(Pt 7):2005–2020.

[45] Kowarschik S, Schollkopf J, Muller T, et al. Yersinia pseudotuberculosis cytotoxic necrotizing factor interacts with glycosaminoglycans. FASEB J. 2021;35(7):e21647.
[46] Keller B, Muhlenkamp M, Deuschle E, et al. Yersinia enterocolitica exploits different pathways to accomplish adhesion and toxin injection into host cells. Cell Microbiol. 2015;17(8):1179–1204.
[47] Nagele V, Heesemann J, Schielke S, et al. Neisseria meningitidis adhesin NadA targets beta1 integrins: functional similarity to Yersinia invasin. J Biol Chem. 2011;286(23):20536–20546.
[48] Bujny MV, Ewels PA, Humphrey S, et al. Sorting nexin-1 defines an early phase of salmonella-containing vacuole-remodeling during salmonella infection. J Cell Sci. 2008;121(Pt 12):2027–2036.
[49] Braun V, Wong A, Landekic M, et al. Sorting nexin 3 (SNX3) is a component of a tubular endosomal network induced by salmonella and involved in maturation of the salmonella-containing vacuole. Cell Microbiol. 2010;12(9):1352–1367.
[50] Liebl D, Qi X, Zhe Y, et al. SopB-mediated recruitment of SNX18 facilitates salmonella typhimurium internalization by the host cell. Front Cell Infect Microbiol. 2017;7:257.
[51] Camilli A, Tilney LG, Portnoy DA. Dual roles of plcA in Listeria monocytogenes pathogenesis. Mol Microbiol. 1993;8(1):143–157.
[52] Gaillard JL, Berche P, Mounier J, et al. In vitro model of penetration and intracellular growth of Listeria monocytogenes in the human enterocyte-like cell line Caco-2. Infect Immun. 1987;55(11):2822–2829.
[53] Marquis H, Doshi V, Portnoy DA. The broad-range phospholipase C and a metalloprotease mediate listeriolysin O-independent escape of Listeria monocytogenes from a primary vacuole in human epithelial cells. Infect Immun. 1995;63(11):4531–4534.
[54] Chang YY, Stévenin V, Duchateau M, et al. Shigella hijacks the exocyst to cluster macropinosomes for efficient vacuolar escape. PLOS Pathog. 2020;16(8):e1008822.
[55] Quigley J, Hughitt VK, Velikovsky CA, et al. The cell wall lipid PDIM contributes to phagosomal escape and host cell exit of mycobacterium tuberculosis. MBio. 2017;8(2).
[56] Muller AJ, Kaiser P, Dittmar KE, et al. Salmonella gut invasion involves TTSS-2-dependent epithelial traversal, basolateral exit, and uptake by epithelium-sampling lamina propria phagocytes. Cell Host Microbe. 2012;11(1):19–32.
[57] Wallis TS, Starkey WG, Stephen J, et al. The nature and role of mucosal damage in relation to Salmonella typhimurium-induced fluid secretion in the rabbit ileum. J Med Microbiol. 1986;22(1):39–49.